# Nonlinear consolidation of vertical drains with coupled radial-vertical flow considering time and depth dependent vacuum pressure

**Si-jie Liu[1], Xue-yu Geng[2], Hong-lei Sun*[3], Yuan-qiang Cai[1], Xiao-dong Pan[4], Li Shi[4].**

**1.** Research Center of Coastal and Urban Geotechnical Engineering, College of Civil Engineering and Architecture, Zhejiang University, Hangzhou, PR China

2. School of Engineering, University of Warwick, Coventry, UK

3. Institute of Disaster Prevention and Reduction Engineering and Protective Engineering, College of Civil Engineering and Architecture, Zhejiang University, Hangzhou 310027, PR China

4. Institute of Geotechnical Engineering, College of Civil Engineering and Architecture, Zhejiang University of Technology, Hangzhou 31000, PR China

**Abstract:** The system of vacuum pressure combined with vertical drains to accelerate soil consolidation is one of the most effective ground improvement methods. The consolidation theories of soft soil improved by vertical drains including void-ratio-dependent compressibility and permeability have been widely applied in practice to predict the consolidation behavior. In this paper, analytical solutions of the consolidation of vertical drains are derived incorporating the loss and propagating stage of vacuum pressure. In addition, special solutions is obtained for the cases of instantaneous surcharge loading and staged surcharge loading, based on the general solution. The solution is verified by ignoring the propagating stage of vacuum pressure formation and comparing it with an existing solution. The effects of vacuum pressure loss and propagating stage combined with other parameters are investigated through the ratio between excess pore water pressure and surcharge loading.

**Key words:** consolidation, vertical drain, vacuum pressure loss, vacuum pressure propagating stage, multi-stage loading

## Introduction

Vacuum pressure and surcharge preloading combined with prefabricated vertical drains is widely used to improve mechanical properties of soft soil [1 - 5]. This method accelerates the consolidation process of soft soil by shortening the drainage path [6] and increasing hydraulic gradient, resulting in lower water content and higher effective stress [7-8]. Compared with applying only surcharge preloading, the application of vacuum pressure reduces the height of the surcharge embankment to achieve the same consolidation settlement. Since the lateral deformation caused by vacuum pressure is compressive and the pore water pressure is smaller than for cases employing only surcharge loading applied, the risk of shear failure of the treated soil can be reduced. Furthermore, the use of vacuum pressure makes the soil improvement cost-effective and environmentally friendly [9-10].

The theory of soil consolidation improved by vertical drains was initially studied by Carrillo [11] and Barron [12] based on an axisymmetric model. Subsequently, Hansbo [6] incorporated the smear effect and well resistance into Barron's model. Zhu and Yin [13] presented a mathematical solution for the consolidation problem of a vertical drain

Correspondence to: Honglei Sun, Institute of Disaster Prevention and Reduction Engineering and Protective Engineering, College of Civil Engineering and Architecture, Zhejiang University, Hangzhou 310027, PR China
Email:sunhonglei@zju.edu.cn

with radial and vertical drainage under ramp loading. The effect of vacuum pressure assisted consolidation was considered as an equivalent surface loading in early studies [14]. However, tests in both laboratory and field confirmed that the vacuum pressure generates negative pore water pressures along the vertical drain and the soil surface [15-16]. Thus, in later studies, the vacuum pressure was usually considered as negative pore water pressure at the drainage boundary in the model.

Further studies about consolidation improved by vacuum pressure showed that the vacuum pressure varied during the consolidation process. Laboratory tests indicated a linear decrease of negative pressure along the drainage path [17]. Some tests found that the decrease happened not only along the vertical direction but also the radial direction [18]. The analytical solutions for consolidation considering the loss of vacuum pressure were proposed. Geng et al. [8] presented a solution including the time-dependent surcharge loading, smear effect and well resistance. Wu et al. [19] solved the radial consolidation problem considering the decrease of vacuum pressure both in the radial and vertical direction. Perera et al. [20] considered the consolidation under vacuum pressure incorporating soil disturbance.

All the aforementioned solutions assumed that the vacuum pressure reaches the design value instantaneously, and keeps constant during consolidation. However, data from some tests indicated that vacuum pressure may propagate gradually at the early stage instead of instantaneously [21]. In this paper, analytical solutions are proposed to consider the effect of vacuum pressure loss and time-dependence. Radial and vertical flow, smear effect, void ratio-dependent compressibility and permeability and time-dependent surcharge preloading are all considered in this solution.

**Basic assumptions, equations and proposed analytical solutions**

Laboratory and field tests have observed that vacuum pressure varied with drain depth and time [9, 21 and 22]. Indraratna et al. [17] assumed linear decrease of negative pore pressure along the drainage depth and unsaturation area around the drain in a numerical model, which made the prediction of consolidation more accurate. The unsaturation area causes the vacuum pressure at the drainage boundary to increase gradually compared to the fully saturated model where vacuum pressure is formed instantaneously at the drainage boundary, which can explain the variation of vacuum pressure with time. As shown in Fig. 1, by fitting the vacuum pressure measured in laboratory tests by Bao et al. (2014) [21] and that measured in the field tests in Taizhou, China by our research group, the vacuum pressure at the soil boundary is investigated to vary with time exponentially, which can be written as

$$p = p_{\mathrm{f}}\left(1-\mathrm{e}^{-k_2 t}\right) \tag{1a}$$

Combining the assumption in previous studies [9, 17] that the vacuum pressure decreases linearly along the drain, the vacuum pressure at the drain boundary is assumed to vary with depth and time in this paper, which can be expressed as

$$p = p_{\mathrm{f}}\left(1-\left(1-k_1\right)\frac{z}{H}\right)\left(1-\mathrm{e}^{-k_2 t}\right) \tag{1b}$$

where $p$ is the vacuum pressure along the drain, $k_1$ is the constant to depict the decrease of vacuum pressure along depth, $k_2$ is the constant to depict the increase of vacuum pressure with time, $p_f$ is the design vacuum pressure, $z$ is the vertical distance from the soil surface, $H$ is the length of drainage path, $t$ is the elapsed time and e is natural logarithm.

The axisymmetric unit cell model is shown in Fig. 2, where $r_w$, $r_s$ and $r_e$ are the radii of the vertical drain, smear zone and the effect zone, respectively; $k_r$ and $k_v$ are the radial and vertical permeable coefficient, respectively; $q$ is the surcharge loading. The following assumptions are adopted in the present study:

(1) To reflect the nonlinearity of permeability and compressibility depending on the void ratio, the following relationship are adopted [23]

$$e = e_0 - C_C \log \frac{\bar{\sigma}'}{\bar{\sigma}'_0} \tag{2a}$$

$$e = e_0 + C_{kh} \log \frac{k_h}{k_{h0}} \tag{2b}$$

$$e = e_0 + C_{kv} \log \frac{k_v}{k_{v0}} \tag{2c}$$

where $C_c$ is the compressive index, $C_{kh}$ and $C_{kv}$ are the radial and vertical permeability index, respectively; $k_h$ and $k_{h0}$ are the radial permeability coefficients of the undisturbed soils at any time and at the initial time, respectively; $k_{v0}$ is the vertical permeability coefficient of the undisturbed soil at initial time; $e$ and $e_0$ are the void ratio at any time and at the initial time, respectively; and $\bar{\sigma}'$ and $\bar{\sigma}'_0$ are the average effective stress at any time and at initial time.

(2) There are several different patterns for distributions of permeable coefficient in smear zone [24]. Since the pattern of permeability distribution influences the consolidation differently from the variation of vacuum pressure, the effect of smear effect is not concerned in this paper. Thus, radial permeability coefficient in smear zone is considered to be constant in this paper for simplification as shown in Fig. 2, which can be expressed as

$$k_r = k_h f(r) \tag{3a}$$

$$f(r) = \begin{cases} 1/\eta, & r_w < r < r_s \\ 1, & r_s < r < r_e \end{cases} \tag{3b}$$

where $\eta = \dfrac{k_{\mathrm{h}}}{k_{\mathrm{r}}\big|_{r=r_{\mathrm{w}}}}$.

(3) The vacuum pressure applied is assumed to vary with time and decreases linearly along the drainage path as in Eq. (1b). The surcharge loading is assumed to be gradually applied on the ground surface.

Following the work by Tang and Onitsuka [25], the governing equation for the nonlinear consolidation of soil improved by vertical drains can be expressed as follows

$$\frac{1}{r}\frac{\partial}{\partial r}\left[\frac{k_{\mathrm{h}} f(r)}{\gamma_w} r \frac{\partial u}{\partial r}\right] + \frac{k_v}{\gamma_w}\frac{\partial^2 \overline{u}}{\partial z^2} = -\frac{\partial \varepsilon_v}{\partial t} \tag{4}$$

where $u$ is the excess pore water pressure, $\overline{u}$ is the average excess pore water pressure in the soil at any depth; $\varepsilon_v$ is the vertical strain of the soil; $\gamma_w$ is the unit weight of water.

(4) In this model, both radial and vertical flow in the soil around the PVDs are considered. The well resistance is ignored.

The boundary and initial conditions are as follows:

$$\begin{cases} r = r_e & \dfrac{\partial u}{\partial r} = 0 \\ r = r_w & u = p_{\mathrm{f}}\left(1-(1-k_1)\dfrac{z}{H}\right)\left(1-\mathrm{e}^{-k_2 t}\right) \\ z = 0 & \overline{u} = p(0) = p_{\mathrm{f}}\left(1-\mathrm{e}^{-k_2 t}\right) \\ z = H & \dfrac{\partial \overline{u}}{\partial z} = 0 \\ t = 0 & u = q(0) = q_{\mathrm{f}} \end{cases} \tag{5}$$

Integrating Eq. (4) and combining it with boundary conditions in the radial direction yields

$$\frac{\partial u}{\partial r} = \frac{\gamma_w}{2k_h}\left(\frac{\partial \varepsilon_v}{\partial t} + \frac{k_v}{\gamma_w}\frac{\partial^2 u}{\partial z^2}\right)\left[\frac{r_e^2}{r f(r)} - \frac{r}{f(r)}\right] \tag{6}$$

By integrating Eq. (6) again and combining it with the boundary conditions, the excess pore pressure in the soil can be derived as:

$$u = \frac{\gamma_w}{2k_h}\left(\frac{\partial \varepsilon_{\mathrm{v}}}{\partial t} + \frac{k_v}{\gamma_w}\frac{\partial^2 \overline{u}}{\partial z^2}\right)\left[r_e^2 A_0(r) - B_0(r)\right] + p_{\mathrm{f}}\left[1-(1-k_1)\frac{z}{l}\right]\left(1-\mathrm{e}^{-k_2 t}\right) \tag{7}$$

where $A_0(r) = \int_{r_w}^{r} \dfrac{\mathrm{d}r}{f(r)\bullet r}$, $B_0(r) = \int_{r_w}^{r} \dfrac{r\mathrm{d}r}{f(r)}$

Based on the equal strain assumption, the average excess pore water pressure in the soil at any depth can be expressed as:

$$\overline{u} = \frac{1}{\pi\left(r_e^2 - r_w^2\right)} \int_{r_w}^{r_e} 2\pi r u \mathrm{d}r \tag{8}$$

Substituting Eq. (7) into Eq. (8) yields:

$$\overline{u} = p_0 \left(1 - \left(1 - k_1\right)\frac{z}{H}\right)\left(1 - \mathrm{e}^{-k_2 t}\right) + \frac{\gamma_w r_e^2 F_a}{2k_m}\left(\frac{\partial \varepsilon_v}{\partial t} + \frac{k_v}{\gamma_w}\frac{\partial^2 \overline{u}}{\partial z^2}\right) \tag{9}$$

where $F_a = \dfrac{2\left(r_e^2 A_1 - B_1\right)}{r_e^2\left(r_e^2 - r_w^2\right)}$, $A_1 = \int_{r_w}^{r_e} r A_0\left(r\right)\mathrm{d}r$, $B_1 = \int_{r_w}^{r_e} r B_0\left(r\right)\mathrm{d}r$

Substituting Eq. (3b) into $A_1$, $B_1$ and $F_a$, the value of $F_a$ can be expressed as

$$F_{\mathrm{a}} = \frac{n^2}{n^2 - 1}\left[\ln n - \frac{3}{4} + \frac{1}{n^2} - \frac{1}{4n^4} + \left(\frac{1}{\eta} - 1\right)\left(\ln s + \frac{1 - s^2}{n^2} + \frac{s^4 - 1}{4n^4}\right)\right] \tag{10}$$

Combining the nonlinear compressive relationship, the rate of deformation can be expressed as

$$\frac{\partial \varepsilon_v}{\partial t} = \frac{1}{1 + e_0}\frac{\partial e}{\partial t} = \frac{1}{1 + e_0}\frac{\partial e}{\partial \overline{\sigma}'}\frac{\partial \overline{\sigma}'}{\partial t} = \frac{-C_c}{(1 + e_0)\ln 10}\frac{1}{\overline{\sigma}'}\frac{\partial \overline{\sigma}'}{\partial t} = -m_{v0}\frac{\sigma_0'}{\overline{\sigma}'}\frac{\partial \overline{\sigma}'}{\partial t} \tag{11}$$

By substituting Eq. (2), (11) into Eq. (9), the average excess pore water pressure can be expressed as:

$$\overline{u} = p_0 \left(1 - \left(1 - k_1\right)\frac{z}{H}\right)\left(1 - \mathrm{e}^{-k_2 t}\right) + \frac{\gamma_w r_e^2 F_a}{2k_{m0}} m_{v0}\left(\frac{\overline{\sigma}'}{\sigma_0'}\right)^{\frac{C_c}{C_{kh}} - 1}\frac{\partial \overline{\sigma}'}{\partial t} + \frac{k_{v0} r_e^2 F_a}{2k_{m0}}\left(\frac{\overline{\sigma}'}{\sigma_0'}\right)^{\frac{C_c}{C_{kh}} - \frac{C_c}{C_{kv}}}\frac{\partial^2 \overline{u}}{\partial z^2} \tag{12}$$

Based on the principle of effective stress, the effective stress can be obtained:

$$\overline{\sigma}' = \overline{\sigma}_0' + q\left(t\right) - \overline{u} \tag{13}$$

Substituting Eq. (13) into Eq. (12) leads to:

$$A\frac{\partial^2 \overline{u}}{\partial z^2} - B\frac{\partial \overline{u}}{\partial t} - \overline{u} = p_{\mathrm{f}}\left(1 - \left(1 - k_1\right)\frac{z}{H}\right)\left(1 - \mathrm{e}^{-k_2 t}\right) - B\frac{\mathrm{d}q\left(t\right)}{\mathrm{d}t} \tag{14}$$

where $A = \dfrac{k_{v0} r_e^2 F_a}{2k_{m0}}\left(\dfrac{\overline{\sigma}'}{\overline{\sigma}_0'}\right)^{\frac{C_c}{C_{kh}} - \frac{C_c}{C_{kv}}}$, $B = -\dfrac{\gamma_w r_e^2 F_a m_{v0}}{2k_{m0}}\left(\dfrac{\overline{\sigma}'}{\overline{\sigma}_0'}\right)^{\frac{C_c}{C_{kh}} - 1}$

The initial stress $\overline{\sigma}'$ varies with time and depth during the consolidation process, which makes the practical differential equations nonlinear and nonhomogeneous. In order to obtain the analytical solution, the approach of Perera et al. [20] and Lenka et al. [23] are used to simplify the equation. The initial and final value of $\overline{\sigma}'$ can be expressed as

$$\begin{cases} t=0 & \bar{\sigma}'=\bar{\sigma}'_0 \\ t=\infty & \bar{\sigma}'=\bar{\sigma}'_0+q_f-\dfrac{1}{2}p_{\mathrm{f}}\left(1+k_1\right) \end{cases} \tag{15}$$

By replacing $\bar{\sigma}'/\bar{\sigma}'_0$ with its average value, the differential equation is reduced to

$$\bar{A}\frac{\partial^2\bar{u}}{\partial z^2}-\bar{B}\frac{\partial\bar{u}}{\partial t}-\bar{u}=p_{\mathrm{f}}\left(1-\left(1-k_1\right)\frac{z}{H}\right)\left(1-\mathrm{e}^{-k_2 t}\right)-\bar{B}\frac{\mathrm{d}q(t)}{\mathrm{d}t} \tag{16}$$

where $\bar{A}=\dfrac{k_{v0}r_e^2F_a}{2k_{m0}}\left(1+\dfrac{q_{\mathrm{f}}-\frac{1}{2}p_{\mathrm{f}}\left(1+k_1\right)}{2\bar{\sigma}'_0}\right)^{\frac{C_c}{C_{kh}}-\frac{C_c}{C_{kv}}}$, $\bar{B}=-\dfrac{\gamma_w r_e^2F_a m_{v0}}{2k_{m0}}\left(1+\dfrac{q_{\mathrm{f}}-\frac{1}{2}p_{\mathrm{f}}\left(1+k_1\right)}{2\bar{\sigma}'_0}\right)^{\frac{C_c}{C_{kh}}-1}$.

Combining with the boundary conditions and initial condition in Eq. (5), the solutions of pore water pressure can be obtained:

$$\bar{u}=p(z,t)+\sum_{m=1}^{\infty}\frac{2}{BH}\left(\frac{BH}{M}q(0)\mathrm{e}^{-\beta_m t}+\frac{H}{M}e^{-\beta_m t}\int_0^t\mathrm{e}^{\beta_m\tau}f(\tau)\mathrm{d}\tau+\frac{H}{M}\mathrm{e}^{-\beta_m t}\int_0^t\mathrm{e}^{\beta_m\tau}B\frac{\mathrm{d}q(\tau)}{\mathrm{d}\tau}\mathrm{d}\tau\right) \tag{17}$$

where $\beta_m=\dfrac{1}{\bar{B}}+\dfrac{\bar{A}}{\bar{B}}\left(\dfrac{M}{H}\right)^2$, $M=\dfrac{2m-1}{2}\pi, m=1,2,3...;$

$$f(\tau)=-Bk_2p_{\mathrm{f}}\mathrm{e}^{-k_2t}-\frac{\left(1-e^{-k_2t}\right)p_{\mathrm{f}}(-1)^{m+1}\left(1-k_1\right)}{M}$$

On the basis of the solution for pore water pressure, the degree of consolidation can be derived as follows

$$\begin{aligned} U_p&=\frac{\Delta\bar{\sigma}'(t)}{\Delta\bar{\sigma}'(\infty)}=\frac{\int_0^H\left[\sigma(z,t)-\bar{u}(z,t)\right]\mathrm{d}z}{\int_0^H\left[\sigma(z,\infty)-\bar{u}(z,\infty)\right]\mathrm{d}z} \\ &=\frac{q(t)-\left[p_{\mathrm{f}}\left(1-\mathrm{e}^{-k_2t}\right)+\frac{1}{M}\sum_{m=1}^{\infty}\frac{2}{BH}\left(\frac{H}{M}\mathrm{e}^{-\beta_m t}\int_0^t\mathrm{e}^{\beta_m\tau}B\frac{\mathrm{d}q(\tau)}{\mathrm{d}\tau}\mathrm{d}\tau+\frac{H}{M}\mathrm{e}^{-\beta_m t}\int_0^t\mathrm{e}^{\beta_m t}f(\tau)\mathrm{d}\tau+\frac{BH}{M}q(0)\mathrm{e}^{-\beta_m t}\right)\right]}{q_{\mathrm{f}}-\left[p_{\mathrm{f}}+\sum_{m=1}^{\infty}\frac{2}{M^2}\left(-\frac{p_0(-1)^{m+1}\left(1-k_1\right)}{BM}\left[\frac{1}{\beta_m}\right]\right)\right]} \end{aligned} \tag{18}$$

# Solutions for several special cases

Based on the proposed solutions for a general time-variable loading, detailed solutions are derived for several special cases: instantaneous loading, single-stage

loading, and multi-stage loading, as shown in Fig.3

(a) Instantaneous loading

As shown in Fig. 3(a), the surcharge preloading is applied instantaneously and keeps constant during the whole process, which can be expressed as follow:

$$q(t)=q_{\mathrm{f}} \tag{19}$$

Substituting Eq. (19) into Eq. (17), the solution for instantaneous surcharge loading considering vacuum pressure varying with time and depth can be obtained:

$$\bar{u}=p_{\mathrm{f}}\left(1-\mathrm{e}^{-k_2 t}\right)+\sum_{m=1}^{\infty}\frac{2}{M}\left(\frac{-k_2 p_{\mathrm{f}}\left[\mathrm{e}^{-k_2 t}-\mathrm{e}^{-\beta_m t}\right]}{\beta_m-k_2}-\frac{p_{\mathrm{f}}(-1)^{m+1}(1-k_1)}{BM}\left[\frac{1-\mathrm{e}^{-\beta_m t}}{\beta_m}-\frac{\mathrm{e}^{-k_2 t}-\mathrm{e}^{-\beta_m t}}{\beta_m-k_2}\right]+q_{\mathrm{f}}\mathrm{e}^{-\beta_m t}\right)\sin\left(\frac{M}{H}z\right) \tag{20}$$

$$U=\frac{q_{\mathrm{f}}-\left[p_{\mathrm{f}}\left(1-\mathrm{e}^{-k_2 t}\right)+\sum_{m=1}^{\infty}\frac{2}{M^2}\left(\frac{-k_2 p_{\mathrm{f}}\left[\mathrm{e}^{-k_2 t}-\mathrm{e}^{-\beta_m t}\right]}{\beta_m-k_2}-\frac{p_{\mathrm{f}}(-1)^{m+1}(1-k_1)}{BM}\left[\frac{1-\mathrm{e}^{-\beta_m t}}{\beta_m}-\frac{\mathrm{e}^{-k_2 t}-\mathrm{e}^{-\beta_m t}}{\beta_m-k_2}\right]+\left(q_{\mathrm{f}}-p(0,0)\right)\mathrm{e}^{-\beta_m t}\right)\right]}{q_{\mathrm{f}}-\left[p_{\mathrm{f}}+\sum_{m=1}^{\infty}\frac{2}{M^2}\left(-\frac{p_{\mathrm{f}}(-1)^{m+1}(1-k_1)}{BM}\left[\frac{1}{\beta_m}\right]\right)\right]} \tag{21}$$

(c) Single-stage loading

As shown in Fig. 3(b), the surcharge preloading is gradually applied by a single-stage pattern. The surcharge pressure increases to the final value in a linear way when $t<t_1$ and keeps constant after $t_1$, which can be described as:

$$q=\begin{cases}\dfrac{t}{t_1}q_{\mathrm{f}} & t\le t_1\\ q_{\mathrm{f}} & t>t_1\end{cases} \tag{22}$$

Substituting Eq. (22) into Eq. (17) and Eq. (18) leads to the solutions.

$$\bar{u}=\begin{cases}p_{\mathrm{f}}\left(1-\mathrm{e}^{-k_2 t}\right)+\sum_{m=1}^{\infty}\frac{2}{M}\left(\frac{-k_2 p_{\mathrm{f}}\left[\mathrm{e}^{-k_2 t}-\mathrm{e}^{-\beta_m t}\right]}{\beta_m-k_2}+\frac{q_1\left(1-\mathrm{e}^{-\beta_m t}\right)}{\beta_m t_1}-\frac{p_{\mathrm{f}}(-1)^{m+1}(1-k_1)}{BM}\left[\frac{1-\mathrm{e}^{-\beta_m t}}{\beta_m}-\frac{\mathrm{e}^{-k_2 t}-\mathrm{e}^{-\beta_m t}}{\beta_m-k_2}\right]\right)\sin\left(\frac{M}{H}z\right) & t<t_1\\ p_{\mathrm{f}}\left(1-\mathrm{e}^{-k_2 t}\right)+\sum_{m=1}^{\infty}\frac{2}{M}\left(\frac{-k_2 p_{\mathrm{f}}\left[\mathrm{e}^{-k_2 t}-\mathrm{e}^{-\beta_m t}\right]}{\beta_m-k_2}+\frac{q_1\left(1-\mathrm{e}^{-\beta_m t_1}\right)}{\beta_m t_1}-\frac{p_{\mathrm{f}}(-1)^{m+1}(1-k_1)}{BM}\left[\frac{1-\mathrm{e}^{-\beta_m t}}{\beta_m}-\frac{\mathrm{e}^{-k_2 t}-\mathrm{e}^{-\beta_m t}}{\beta_m-k_2}\right]\right)\sin\left(\frac{M}{H}z\right) & t>t_1\end{cases} \tag{23}$$

$$U=\begin{cases}\dfrac{\dfrac{q_f}{t_1}t-\left[p_f\left(1-e^{-k_2t}\right)+\sum_{m=1}^{\infty}\dfrac{2}{M^2}\left(\dfrac{-k_2p_f\left[e^{-k_2t}-e^{-\beta_mt}\right]}{\beta_m-k_2}+\dfrac{q_f\left(1-e^{-\beta_mt}\right)}{\beta_mt_1}-\dfrac{p_f(-1)^{m+1}(1-k_1)}{BM}\left[\dfrac{1-e^{-\beta_mt}}{\beta_m}-\dfrac{e^{-k_2t}-e^{-\beta_mt}}{\beta_m-k_2}\right]\right)\right]}{q_f-\left[p_f\left(1-e^{-k_2t}\right)+\sum_{m=1}^{\infty}\dfrac{2}{M^2}\left(\dfrac{q_f\left(1-e^{-\beta_mt_1}\right)}{\beta_mt_1}-\dfrac{p_f(-1)^{m+1}(1-k_1)}{BM}\left[\dfrac{1}{\beta_m}\right]\right)\right]} & t<t_1\\ \dfrac{\dfrac{q_f}{t_1}t-\left[p_f\left(1-e^{-k_2t}\right)+\sum_{m=1}^{\infty}\dfrac{2}{M^2}\left(\dfrac{-k_2p_f\left[e^{-k_2t}-e^{-\beta_mt}\right]}{\beta_m-k_2}+\dfrac{q_f\left(1-e^{-\beta_mt_1}\right)}{\beta_mt_1}-\dfrac{p_f(-1)^{m+1}(1-k_1)}{BM}\left[\dfrac{1-e^{-\beta_mt}}{\beta_m}-\dfrac{e^{-k_2t}-e^{-\beta_mt}}{\beta_m-k_2}\right]\right)\sin\left(\dfrac{M}{H}z\right)\right]}{q_f-\left[p_f\left(1-e^{-k_2t}\right)+\sum_{m=1}^{\infty}\dfrac{2}{M^2}\left(\dfrac{q_f\left(1-e^{-\beta_mt_1}\right)}{\beta_mt_1}-\dfrac{p_f(-1)^{m+1}(1-k_1)}{BM}\left[\dfrac{1}{\beta_m}\right]\right)\right]} & t>t_1\end{cases} \tag{24}$$

(d) Multi-stage loading

As is shown in Fig.3(c), surcharge preloading is loaded stage by stage when the soil is so soft that can't support a large surcharge loading instantaneously. Compared with other methods, this method reduces the risk of the ground failure. For simplicity, in each stage, the loading is assumed to increase linearly in each stage which can be expressed as

$$\begin{aligned}&t=t_0=0,\quad q(0)=0\\ &t>0,\quad q(t)=\begin{cases}q_{i-1}+\dfrac{(q_i-q_{i-1})}{\left(t_{(2i-1)}-t_{(2i-2)}\right)}(t-t_{2i-2}), & t_{2i-2}<t<t_{2i-1}\quad (i=1,2,3...)\\ q_i, & t_{2i-1}<t<t_{2i}\end{cases}\end{aligned} \tag{25}$$

Where $i$ is the $i$th stage of loading; and $q_i$ is the final loading of each increase stage. Substituting Eq. (25) into Eq. (17) and Eq. (18) leads to the solution:

$$\bar{u}=\begin{cases}p_0\left(1-e^{-k_2t}\right)+\sum_{m=1}^{\infty}\dfrac{2}{M}\left(\begin{array}{l}-\dfrac{k_2p_0\left(e^{-k_2t}-e^{-\beta_mt}\right)}{\beta_m-k_2}\\ +\sum_{j=1}^{i-1}\dfrac{q_j-q_{j-1}}{t_{2j-1}-t_{2j-2}}\dfrac{e^{-\beta_m\left(t-t_{2j-1}\right)}-e^{-\beta_m\left(t-t_{2j-2}\right)}}{\beta_m}+\dfrac{q_i-q_{i-1}}{t_{2i-1}-t_{2i-2}}\dfrac{1-e^{-\beta_m\left(t-t_{2i-2}\right)}}{\beta_m}\\ -\dfrac{p_0(-1)^{m+1}(1-k_1)}{MB}\left(\dfrac{1-e^{-\beta_mt}}{\beta_m}-\dfrac{e^{-k_2t}-e^{-\beta_mt}}{\beta_m-k_2}\right)\end{array}\right)\sin\left(\dfrac{M}{H}z\right) & t_{2i-2}<t<t_{2i-1}\\ p_0\left(1-e^{-k_2t}\right)+\sum_{m=1}^{\infty}\dfrac{2}{M}\left(\begin{array}{l}-\dfrac{k_2p_0\left(e^{-k_2t}-e^{-\beta_mt}\right)}{\beta_m-k_2}\\ +\sum_{j=1}^{i}\dfrac{q_j-q_{j-1}}{t_{2j-1}-t_{2j-2}}\dfrac{e^{-\beta_m\left(t-t_{2j-1}\right)}-e^{-\beta_m\left(t-t_{2j-2}\right)}}{\beta_m}\\ -\dfrac{p_0(-1)^{m+1}(1-k_1)}{MB}\left(\dfrac{1-e^{-\beta_mt}}{\beta_m}-\dfrac{e^{-k_2t}-e^{-\beta_mt}}{\beta_m-k_2}\right)\end{array}\right)\sin\left(\dfrac{M}{H}z\right) & t_{2i-1}<t<t_{2i}\end{cases} \tag{26}$$

In order to obtain the numeral solution, a simple MATLAB program has been developed based on the analytical solution for the special cases. The cases in the following verification and parameter analysis sections are calculated using the program.

**Verification of the proposed solution**

If $k_2\to+\infty$, which means both the vacuum pressure and surcharge loading reach the design magnitude instantaneously, the solution for single stage loading reduces to

$$U=\begin{cases}\dfrac{\dfrac{q_{\mathrm{f}}}{t_1}t-\left[p_{\mathrm{f}}+\sum_{m=1}^{\infty}\dfrac{2}{M^2}\left(\dfrac{q_{\mathrm{f}}\left(1-\mathrm{e}^{-\beta_m t}\right)}{\beta_m t_1}-\dfrac{p_{\mathrm{f}}(-1)^{m+1}(1-k_1)\left(1-\mathrm{e}^{-\beta_m t}\right)}{BM\beta_m}\right)\right]}{q_{\mathrm{f}}-\left[p_{\mathrm{f}}+\sum_{m=1}^{\infty}\dfrac{2}{M^2}\left(\dfrac{q_{\mathrm{f}}\left(1-\mathrm{e}^{-\beta_m t_1}\right)}{\beta_m t_1}-\dfrac{p_{\mathrm{f}}(-1)^{m+1}(1-k_1)}{BM}\left[\dfrac{1}{\beta_m}\right]\right)\right]} & t<t_1\\ \dfrac{\dfrac{q_{\mathrm{f}}}{t_1}t-\left[p_{\mathrm{f}}+\sum_{m=1}^{\infty}\dfrac{2}{M^2}\left(\dfrac{q_{\mathrm{f}}\left(1-\mathrm{e}^{-\beta_m t_1}\right)}{\beta_m t_1}-\dfrac{p_{\mathrm{f}}(-1)^{m+1}(1-k_1)\left(1-\mathrm{e}^{-\beta_m t}\right)}{BM\beta_m}\right)\sin\left(\dfrac{M}{H}z\right)\right]}{q_{\mathrm{f}}-\left[p_{\mathrm{f}}+\sum_{m=1}^{\infty}\dfrac{2}{M^2}\left(\dfrac{q_{\mathrm{f}}\left(1-\mathrm{e}^{-\beta_m t_1}\right)}{\beta_m t_1}-\dfrac{p_{\mathrm{f}}(-1)^{m+1}(1-k_1)}{BM}\left[\dfrac{1}{\beta_m}\right]\right)\right]} & t>t_1\end{cases}$$

(27)

The solution here has the same form as the case where only vacuum pressure loss along the depth is considered [25]. One case calculated by Guo (2010) [26] is adopted here to compare with the proposed solution, which is shown in Fig. 4, where $T_{\mathrm{h}}=c_{\mathrm{h}}t/\left(4r_{\mathrm{e}}^2\right)$, $T_{\mathrm{c}}=c_{\mathrm{h}}t_1/\left(4r_{\mathrm{e}}^2\right)$. It can be seen that solution in this paper fits well with that in Guo's, which proves the reliability of the derivation in this paper.

## Parametric analysis

To study the effect of vacuum pressure variation on the consolidation behavior, parameter analyses are conducted based on the solutions proposed in the last section. The pore water pressure in the analysis is the average value of the soil in different depth and radius, which is defined as follows.

$$\overline{u}_{\mathrm{rz}}=\frac{\int_0^H\int_{r_{\mathrm{w}}}^{r_{\mathrm{e}}}\overline{u}\,\mathrm{d}r\mathrm{d}z}{\pi\left(r_{\mathrm{e}}^2-r_{\mathrm{w}}^2\right)H} \tag{28}$$

### Effect of vacuum pressure propagating exponent, $k_2$

The vacuum pressure is considered propagating exponentially at the early stage due to the unsaturation area and then reaches the designed magnitude. $k_2$ is used here to represent the speed of vacuum pressure propagating. The larger $k_2$ is, the faster the vacuum pressure attains the design value. Fig. 5 shows the influence of the propagating exponent $k_2$ on the consolidation process. Based on Eq. (1), the solution can be reduced to cases without vacuum pressure and with instantaneous vacuum pressure when $k_2$=0 and $k_2$=+∞ respectively.

It can be observed in Fig. 5 that an increase of $k_2$ accelerates the development of consolidation. However, since the difference between $k_2$=0.2 and 0.6 is obviously larger than that between 0.6 and 1.0, this influence reduces nonlinearly with the increase of $k_2$, especially when the magnitude of $k_2$ is over 1. Thus, the effect of the vacuum propagating stage can be neglected in the prediction of the consolidation behavior when

the value of $k_2$ is larger than 1, which indicates that the vacuum pressure attains the design value within 3 days. What's more, the differences of $u_0/q_f$ between the gradual vacuum pressure and instantaneous vacuum pressure increase first and then decrease. The maximum difference appears later as $k_2$ decreases, because a smaller $k_2$ means a longer time spent to reach the designed vacuum pressure, which makes the difference increase. In Fig.5, it can be seen that negative pore water pressure with different $k_2$ has the same final magnitude, so $k_2$ has no influence on the final settlement.

Fig. 6 compares the influence of the vacuum pressure propagating stage for different final vacuum pressure on the consolidation behavior. It can be investigated that the effect of $k_2$ varies with the magnitude of vacuum pressure. The maximum differences of $u/q_f$ caused by this parameter for -60kPa, -80kPa and –100kPa are 0.09, 0.12 and 0.15. Thus, it can be concluded that the influence of $k_2$ on consolidation increases with the value of designed vacuum pressure. This can be explained by the fact that it takes more time for the vacuum pressure to reach a larger magnitude of the designed value, so the difference increases within a longer time.

The dissipation of pore water pressure for different loading process is shown in Fig. 7 to investigate the effect of $k_2$. It is shown that $k_2$=0.2 slows down the dissipation of pore water pressure and increases its maximum value no matter what the patterns of surcharge loading applied. It is easy to see in Fig.7 that the maximum pore water pressure decreases with gradual loading applied which was also shown in [27]. Compared with cases where only surcharge loading is applied shown in Fig. 7 (a), the excess pore pressure in the cases with vacuum pressure is much smaller than those without vacuum pressure. The final pore water pressures for three patterns of surcharge loading and different $k_2$ are the same, which means the same soil improvement effect can be obtained. However, the development of consolidation degree slows down for gradual surcharge loading. Fig. 8 shows the effect of different loading speed combined with the influence of $k_2$. When $t_1$=10, the pore water pressure tends to increase first and then decrease, while for $t_1$=30 or 50, the increase is not so evident. Thus, the pore water pressure turns out to increase only when applying the surcharge loading fast. It can be seen that the difference lasts longer when the surcharge loading is applied faster, because the corresponding ratio of vacuum pressure to the design value for $t$=10, 30, 50 is 0.86, 1.0 and 1.0 respectively when $k_2$=0.2. Thus, for $t_1$=10 days, the vacuum pressure is still increasing after finishing the surcharge loading application. While for $t_1$=30 days and 50 days, the vacuum pressure has already reached the design value when the surcharge loading application is finished.

**Effects of vacuum pressure loss along depth**

Fig. 9 shows the dissipation of excess pore water pressure with various degree of vacuum pressure loss along the drainage path. From Fig. 9, it can be seen that degree of vacuum pressure loss affects the consolidation significantly. The maximum difference between $k_1$=0 and $k_1$=1 at the bottom may reach 50%. Moreover, a smaller vacuum pressure loss always results in a faster dissipation of the pore water pressure. The loss of vacuum affects the consolidation behaviors in two ways. On one hand, it makes the hydraulic gradient in the vertical direction increase. On the other hand, it

leads to the decrease of hydraulic gradient in the radial direction. Since the flow in the radial direction plays a more important role in the process of excess pore water dissipation, the total effect of the vacuum pressure loss is the decrease of pore water dissipation. Also, it can be indicated that the difference between results for different degrees of vacuum pressure loss increases with the development of consolidation, because the hydraulic gradient is higher for the small degree of loss in the whole process, leading to more pore water flowing out. As a result, it can be deduced that the increase of degree of vacuum pressure loss leads to the decrease in the final settlement. Fig.10 shows the influence of vacuum pressure loss combined with the length of drainage path on the dissipation of pore water pressure. It can be seen that the effect of drainage path length is much smaller than the degree of vacuum pressure loss. Thus, the dissipation of pore water pressure is equal no matter how long the drainage path is.

Fig. 11 shows the effect of degree of vacuum pressure loss combined with the final value of vacuum pressure. It can be seen that the influence of vacuum pressure loss varies with the maximum value of vacuum pressure. That is, increase of the magnitude of vacuum pressure raises the influence of vacuum pressure loss degree on the dissipation of pore water pressure, because the magnitude of negative pore water pressure increases as the final vacuum pressure increases.

**Conclusion**

This paper derives an analytical solution for the nonlinear consolidation of a vertical drain with coupled radial-vertical flow by considering the variation of vacuum pressure, the variation of soil compressibility and permeability with void ratio. Then detailed solutions are provided for instantaneous, single-stage, and multi-stage loading. The present solution is verified by a previous study. Finally, the nonlinear consolidation behavior of a vertical drain is investigated using parametric analysis, and the results show that

(1) The exponentially increasing stage of vacuum pressure affects the consolidation significantly, especially when the exponent is small. The consolidation speed increases nonlinearly with the increase of this exponent. When the propagating factor is over 1, the behavior of consolidation has little difference, so the effect of variation with time can be ignored.
(2) Application of multi-stage surcharge loading and vacuum pressure reduces the pore water pressure in the consolidation process and the influence of the vacuum propagating effect lasts a longer time when surcharge loading is applied faster.
(3) The vacuum pressure loss along the drain slows the dissipation of pore water pressure, and the influence increases with the increase of vacuum pressure loss. The vacuum loss influences the flow in radial direction more than that in the vertical direction.

**Acknowledgment**

This work is supported by the National Key R&D Program of China (Grant No. 2016YFC0800200), the Projects of International Cooperation and Exchanges NSFC (Grant No. 51620105008), National Science Foundation for Young Scientists of China (Grant No. 51608482) and National Natural Science Foundation of China (Grant No. 51478424).

**Reference**

[1] Mohamedelhassan E, Shang J Q. Vacuum and surcharge combined one-dimensional consolidation of clay so. [J]. Canadian Geotechnical Journal, 2002, 39(5):1126-1138(13).

[2] Chu J, Yan S W, Yang H. Soil improvement by the vacuum preloading method for an oil storage station [J]. Géotechnique, 2000, 50(6):625-632.

[3] Zhuang Y, Cui X Y. Evaluation of Vacuum Preloading with Vertical Drains as a Soft Soil Improvement Measure [J]. Soil Mechanics & Foundation Engineering, 2016, 53(3):210-217.

[4]. Geng X, Yu H S. A large-strain radial consolidation theory for soft clays improved by vertical drains [J]. Géotechnique, 2017, 67(11):1-9.

[5] Zhou W H, Lok M H, Zhao L S, et al. Analytical solutions to the axisymmetric consolidation of a multi-layer soil system under surcharge combined with vacuum preloading[J]. Geotextiles & Geomembranes, 2017.

[6] Hansbo S. Consolidation of fine-grained soils by prefabricated drains [J]. Proc.of.the.icsmfe, 1980, 3:677-682.

[7] Chai, J. C., Hong, Z. S., Shen, S. L. Vacuum-drain consolidation induced pressure distribution and ground deformation [J]. Geotextiles and Geomembranes, 2010, 28(6), 525-535.

[8] Geng X Y, Indraratna B, Rujikiatkamjorn C. Analytical Solutions for a Single Vertical Drain with Vacuum and Time-Dependent Surcharge Preloading in Membrane and Membraneless Systems[J]. International Journal of Geomechanics, 2012, 10(1):27-42.

[9] Indraratna B, Rujikiatkamjorn C, Sathananthan I. Analytical and numerical solutions for a single vertical drain includi. [J]. Canadian Geotechnical Journal, 2005, 42(4):994-1014.

[10] Indraratna B, Rujikiatkamjorn C, Geng X, et al. Performance and prediction of vacuum combined surcharge consolidation at Port of Brisbane[C]// Faculty of Engineering - Papers. 2011.

[11] Carrillo N. Simple Two and Three Dimensional Case in the Theory of Consolidation of Soils [J]. Studies in Applied Mathematics, 1942, 21(1-4):1–5.

[12] Barron R A. Consolidation of fine grained soils by drain wells [J]. Trans of Asce, 1948, 113(118):324-360.

[13] Zhu G, Yin J H. Consolidation of soil with vertical and horizontal drainage under ramp load [J]. Géotechnique, 2001, 51(4):361-367.

[14] Kjellman, W. 1952. Consolidation of clayey soils by atmospheric pressure. Proceedings of a Conference on Soil Stabilisation. Massachusetts Institute of Technology, Boston, 18-20 June 1952. MIT Press. pp. 258-263

[15] Shang J Q, Tang M, Miao Z. Vacuum preloading consolidation of reclaimed land: a case study [J]. Canadian Geotechnical Journal, 1998, 35(5):740-749.

[16] Tang M, Shang J Q. Vacuum preloading consolidation of Yaoqiang Airport runway [J]. Géotechnique, 2000, 50(6):613-623.

[17] Indraratna B, Bamunawita C, Khabbaz H. Numerical modeling of vacuum preloading and field applications [J]. Canadian Geotechnical Journal, 2004,

41(6):1098-1110.
[18] Li N., Li X. F., Wu Y. D. Experimental study on relationship between vacuum pressure transfer law and permeability coefficient [J]. Subgrade Engineering, 2011 (4): 101 - 103.
[19] Yuedong Wu, Hongsheng Wu, Luo R, et al. Analytical solutions for vacuum preloading consolidation considering vacuum degree attenuation and change of permeability coefficient in smear zones[J]. Journal of Hohai University, 2016. (in Chinese)
[20] Perera, D., Indraratna, B., Leroueil, S., Rujikiatkamjorn, C., & Kelly, R. Analytical model for vacuum consolidation incorporating soil disturbance caused by mandrel-driven drains [J]. Canadian Geotechnical Journal, 2017, 54(4), 547-560.
[21] Bao S F, Yan L, Dong Z L, et al. Causes and countermeasures for vacuum consolidation failure of newly-dredged mud foundation [J]. Chinese Journal of Geotechnical Engineering, 2014, 36(7):1350-1359.
[22] Chai J C, Carter J P, Hayashi S. Ground Deformation Induced by Vacuum Consolidation [J]. Journal of Geotechnical & Geoenvironmental Engineering, 2005, 131(131):1552-1561.
[23] Lekha K R, Krishnaswamy N R, Basak P. Consolidation of Clay by Sand Drain under Time-Dependent Loading[J]. Journal of Geotechnical & Geoenvironmental Engineering, 1998, 124(1):91-94.
[24] Xie K H, Lu M M, Liu G B. Equal strain consolidation for stone columns reinforced foundation [J]. International Journal for Numerical & Analytical Methods in Geomechanics, 2010, 33(15):1721-1735.
[25] Tang, X., Onitsuka, K. Consolidation by vertical drains under time-dependent loading [J]. International Journal for Numerical and Analytical Methods in Geomechanics, 2000, 24(9), 739-751.
[26] Guo Biao. Analytical study on axisymmetric consolidation theory of ground with vertical drains [D]. Hangzhou: Zhejiang University, 2010. (In Chinese).
[27] Lu M, Wang S, Sloan S W, et al. Nonlinear consolidation of vertical drains with coupled radial–vertical flow considering well resistance[J]. Geotextiles & Geomembranes, 2015, 43(2):182-189.

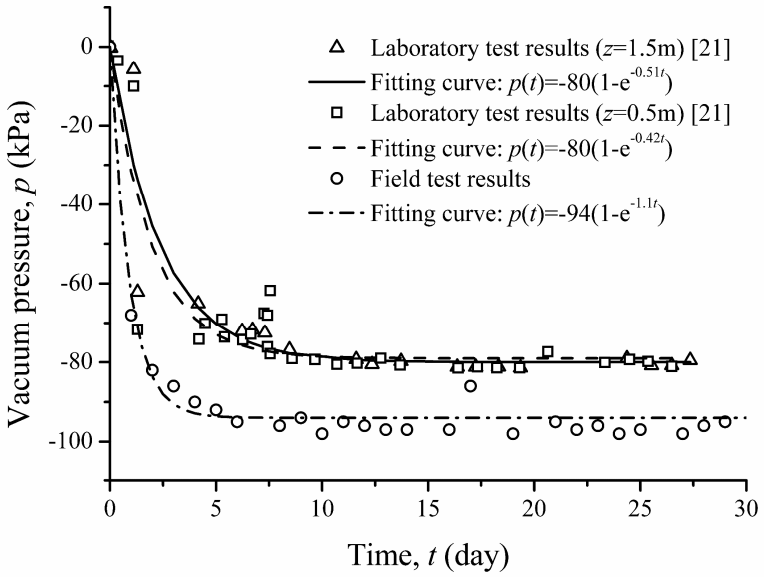


Fig. 1 Propagating properties of vacuum pressure measured in tests

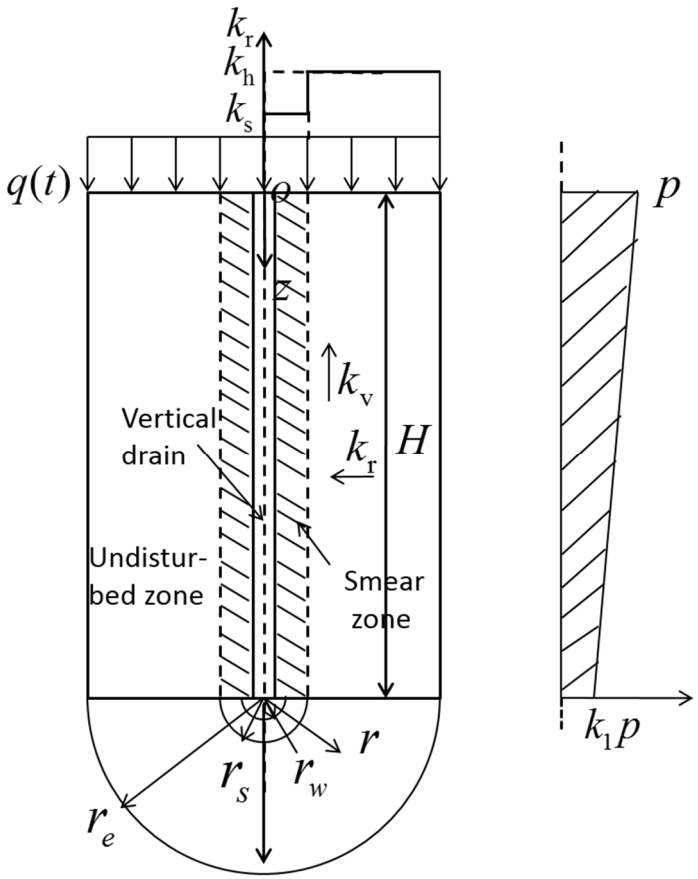


Fig. 2 Analysis scheme of unit cell with vertical drain

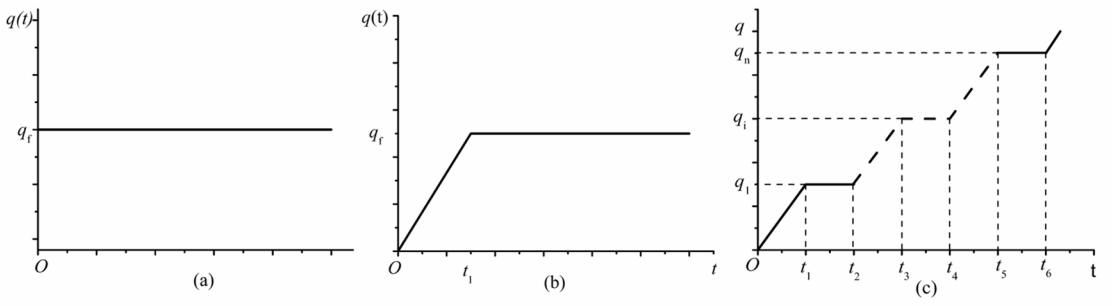


Fig. 3 Surcharge loading schemes

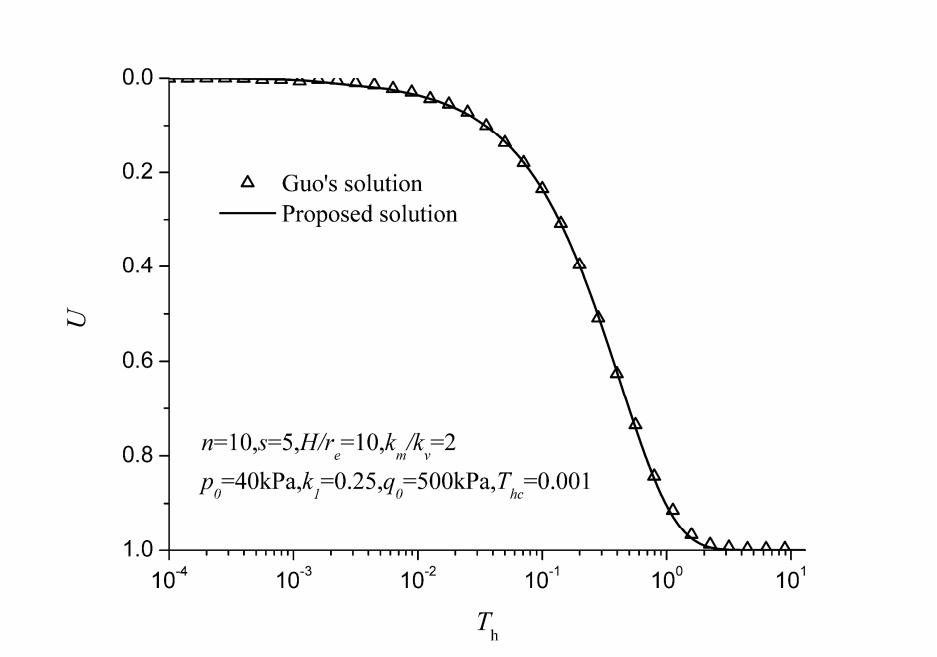


Fig. 4 Comparison between Guo's solution and author's solution

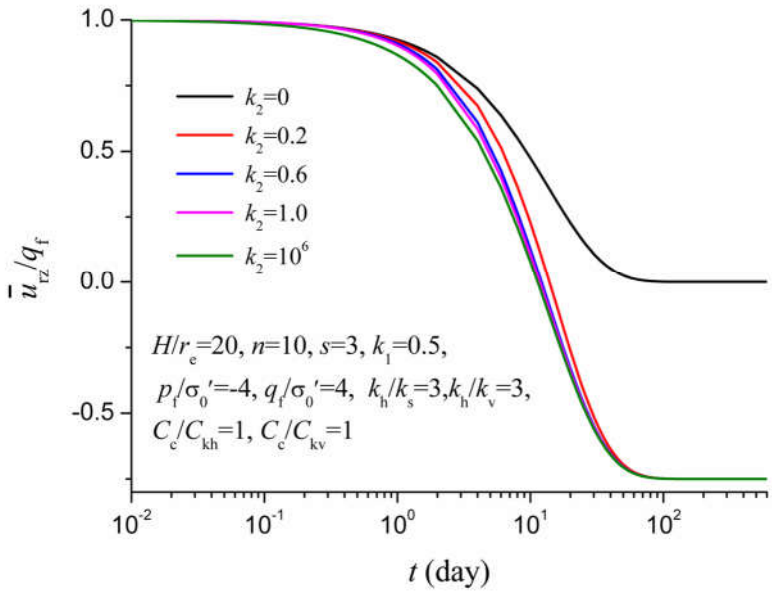


Fig. 5 Effect of vacuum pressure propagating with time on the dissipation of pore water pressure

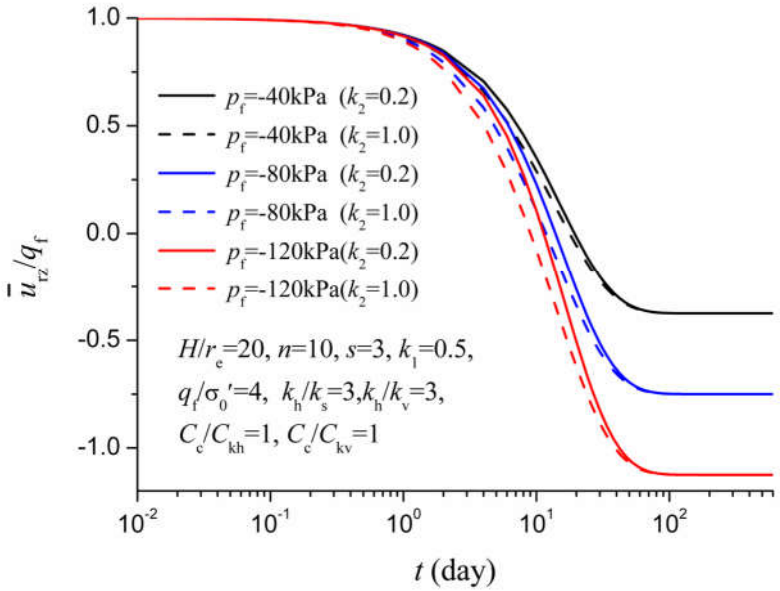


Fig. 6 Effect of vacuum pressure propagating with time under different magnitudes of loading on the dissipation of pore water pressure

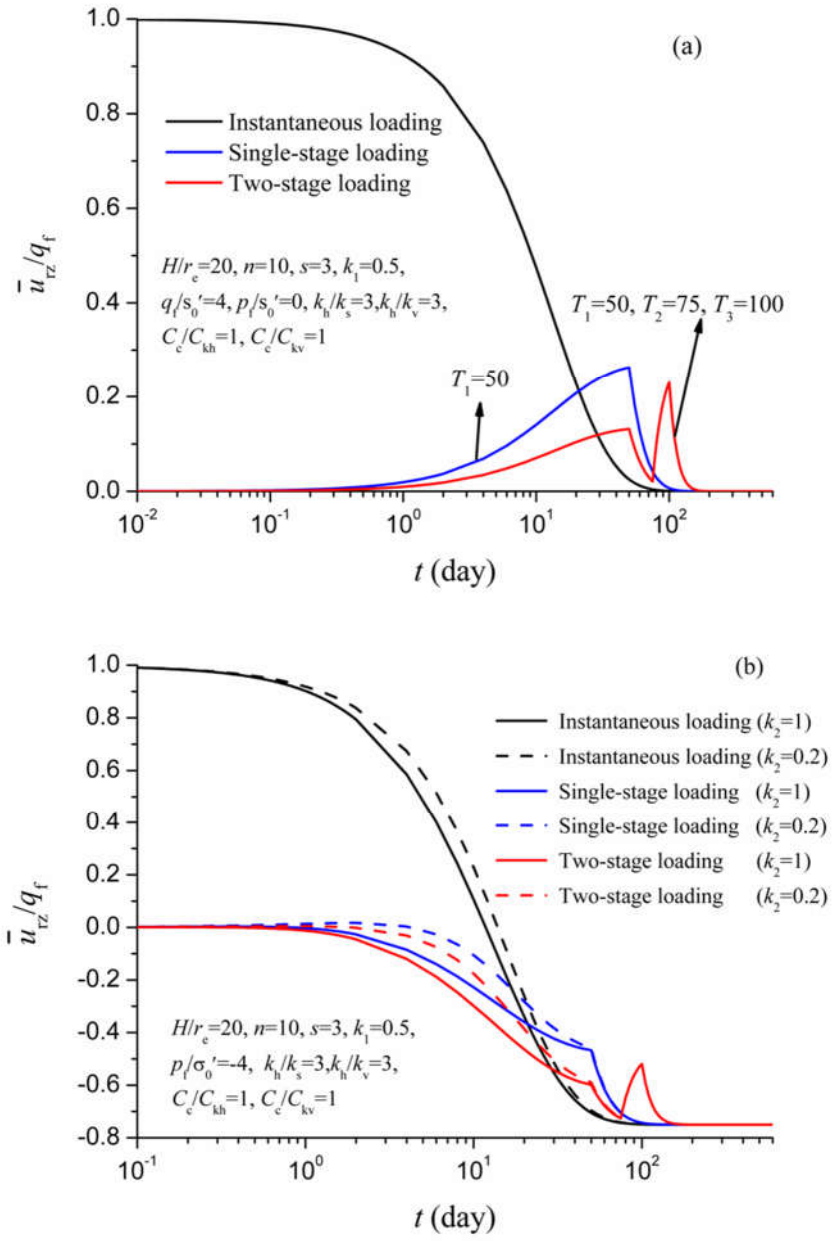


Fig. 7 Effect of loading process on the dissipation of pore water pressure (a) without vacuum pressure (b) with vacuum pressure propagating with time

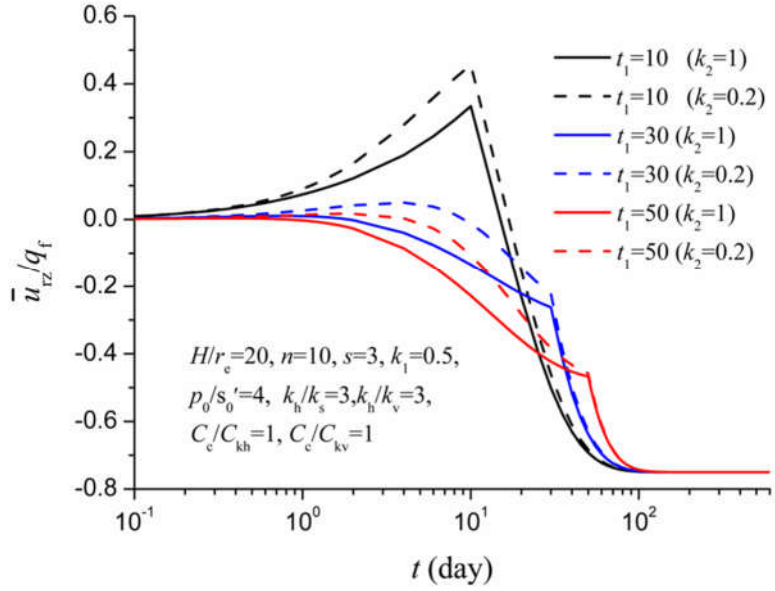


Fig. 8 Effect of vacuum pressure propagating with time on the dissipation of pore water pressure under different loading speed

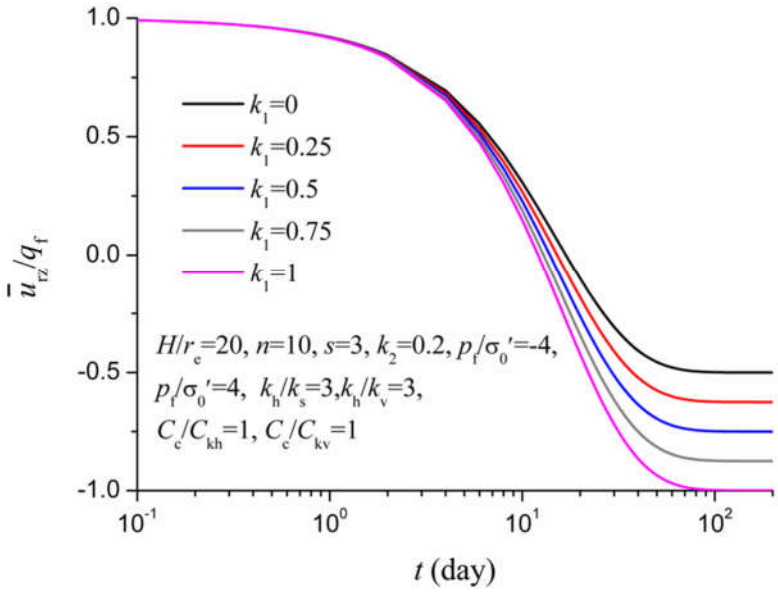


Fig. 9 Effect of vacuum pressure loss along depth on the dissipation of pore water pressure

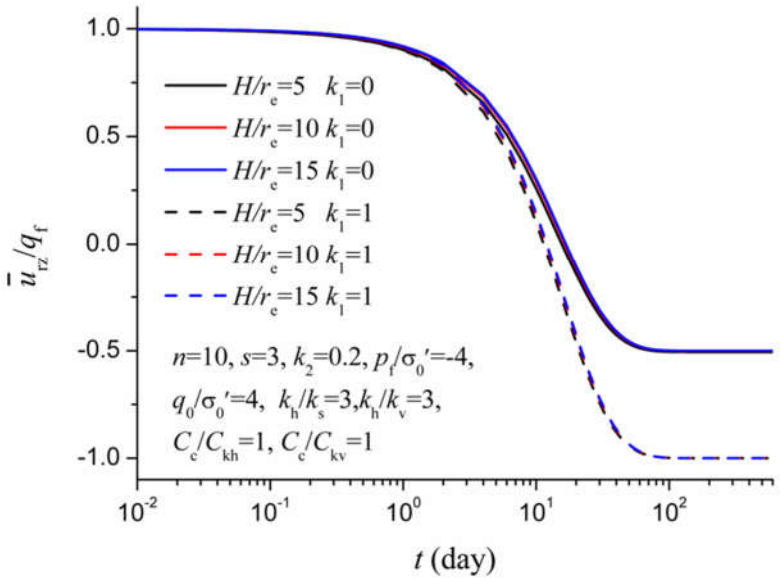


Fig. 10 Effect of vacuum pressure loss combined with different drainage length along depth on the dissipation of pore water pressure

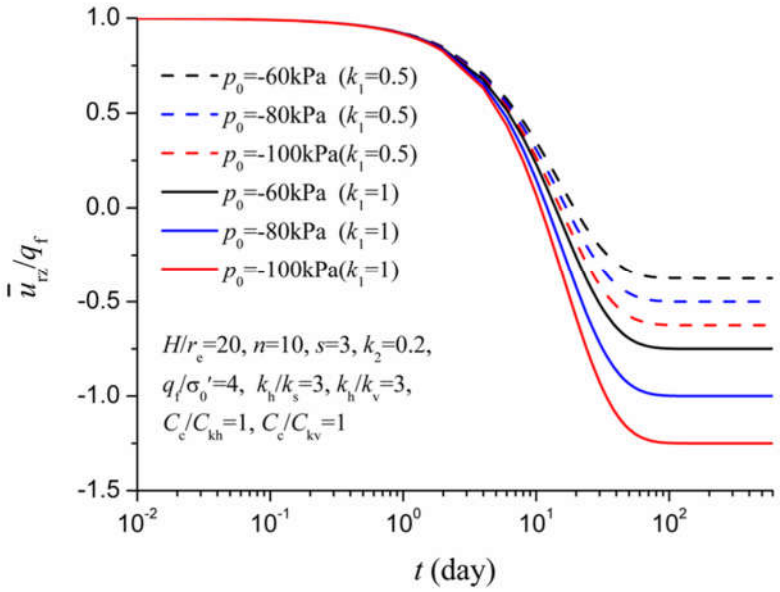


Fig. 11 Effect of vacuum pressure loss combined with different magnitudes loading along depth on the dissipation of pore water pressure